PERGAMON

Journal of Structural Geology 21 (1999) 1751–1771

JOURNAL OF STRUCTURAL GEOLOGY

www.elsevier.nl/locate/jstrugeo

# Determination of stress directions from plagioclase fabrics in high grade deformed rocks (Além Paraíba shear zone, Ribeira fold belt, southeastern Brazil)

Marcos Egydio-Silva[a,*], David Mainprice[b]

[a]*Instituto de Geociências da Universidade de São Paulo, Cep: 05422-970, C. P. 11348, São Paulo, Brazil*
[b]*Laboratoire de Tectonophysique, Université Montpellier II, Place Eugene Bataillon, 34095 Montpellier cedex 5, France*

Received 26 August 1997; accepted 15 June 1999

**Abstract**

A new method to determine stress directions using the preferential orientation of plagioclase mechanical twins has been applied to high-temperature mylonitic rocks from the Além Paraíba shear zone, Ribeira fold belt, southeastern Brazil. We have measured the lattice-preferred orientation of plagioclase grains and calculated the orientation of the stress axes possible for the observed twin orientations. The maximum compressive stress direction ($\sigma_1$), determined for all studied samples, is a function of the mechanical twin orientations of a number of distinct plagioclase populations. The $\sigma_1$ direction is generally subperpendicular to the (010) plane. The statistical treatment for most of the plagioclase grains examined for each sample shows that $\sigma_1$ is almost perpendicular to the foliation plane, suggesting a significant coaxial component in the deformation process of these rocks. 

## 1. Introduction

Most methods for determining the principal stress axes in deformed rocks involve dynamic analysis of twin gliding and of extinction bands produced by inhomogeneous translation glide in crystals (Carter and Raleigh, 1969). These methods, beginning with the techniques of Turner (1953) for dynamic analysis of calcite twins, have been developed based on experimental results on single crystals. Stress direction determination using mechanical twin preferred orientations in rocks naturally deformed at high temperatures in the lower crust has not been attempted so far.

Analysis of the stresses involved in rock deformation is not a simple matter. A number of techniques are available which enable determination of principal stress directions (e.g. Carter and Raleigh, 1969; Laurent and Tourneret, 1990; Tourneret and Laurent, 1990). These authors have shown that structures resulting from intracrystalline flow in calcite, dolomite, quartz, micas, orthopyroxenes, olivine, plagioclases and other common rock-forming minerals may be used to infer the principal stress axes. Similarly, it is theoretically possible to determine the maximum stress direction from the orientation of mechanical albite and pericline twins in rocks deformed at high temperature (Borg and Heard, 1970; Lawrence, 1970).

The purpose of this paper is to apply this theoretical approach to determine the maximum principal stress orientation in high-grade mylonites. For this objective we have investigated the lattice-preferred orientations of plagioclase and calculated the possible directions of the stress axes for the observed twin orientations in deformed rocks from a high-temperature ductile shear zone (Além Paraíba shear zone) of the Neoproterozoic Ribeira belt in southeastern Brazil.

* Corresponding author.
*E-mail address:* megydios@spider.usp.br (M. Egydio-Silva)

0191-8141/99/$ - see front matter 
PII: S0191-8141(99)00121-2

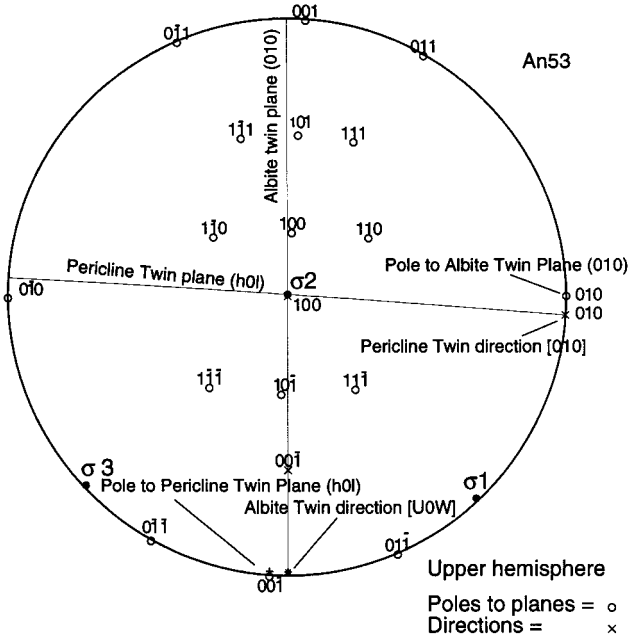


Fig. 1. Stereogram of the geometric elements of mechanical albite and pericline twins in $An_{53}$ and the compression axis or optimum position of $\sigma_1$ in order to induce twin gliding according to one or both laws.

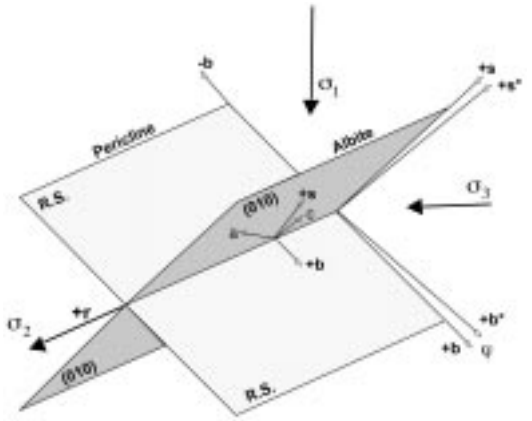


Fig. 2. Tridimensional arrangement of the geometric elements of mechanical albite and pericline twins, and the compression axis relative to the mechanical twinning. The maximum compressive stress is placed where the senses of shear of albite and pericline twinning are positive and negative, respectively. Glide lines $b$ and $s$, and glide planes, RS (rhombic section) and (010), for pericline and albite twins; **r**, the rhombic line is perpendicular to **b**, $\mathbf{b}^*$, $\mathbf{s}^*$. The obliquity is $\varphi = \mathbf{b} \wedge \mathbf{b}^* = \mathbf{s} \wedge \mathbf{s}^*$.

## 2. Theoretical background

The origin of plagioclase twinning in naturally deformed rocks has been the subject of much discussion and investigation. Two types of twinning are possible in feldspars, by pseudomerohedry and by lattice pseudomerohedry. Only albite and pericline twins result from pseudomerohedry, all other twinning in feldspars is by lattice pseudomerohedry (Smith and Brown, 1988).

Buerger (1945) classified twins as growth, transformation and glide (or mechanical twins). A number of works, including Emmons and Gates (1943), Muir (1955), and Gay and Bown (1956) recognized the possibility that twinning (albite and pericline laws) may develop not only during growth but also during solid phase transformations and gliding (mechanical origin), as first suggested by Van Werveke (1883, in Borg and Handin, 1966). Crystal morphology is difficult to use as a criterion to distinguish among the various mechanisms by which twinning may form.

Borg and Heard (1970) performed high-pressure experiments on plagioclase specimens of various compositions, and observed that mechanical twinning only occurred in specimens deformed above 800°C with confining pressures of about 800 to 1000 MPa. They emphasized that if the observed albite and pericline twins are mechanical in origin, it is possible to deduce the orientation of the principal stresses that produced twinning. By analogy with the method developed by Turner (1953), for mechanically twinned calcite, a maximum compression axis can be graphically determined for each twinned plagioclase grain.

The resolved shear stress must be at a maximum in the positive sense for the twin system. In the case of albite and pericline mechanical twins, this occurs for compression axes at 45° to slip plane (010) and rhombic section and glide line. It should also lie in quadrants defined by either (001) and $(0\bar{1}0)$, or by $(00\bar{1})$ and (010) (Fig. 1).

Deformation due to twin gliding may be simplistically regarded as homogeneous simple shear between one part of a crystal structure (albite twin) and the composition plane (Fig. 2). In this simple model, each atom in the layer above the composition plane has moved some fixed fraction (depending on the crystal structure) of an integral atomic translation (Carter and Raleigh, 1969). If we consider only mechanical twins, the composition plane cannot be a symmetry plane of the crystal, and there is only one direction of twin gliding according to a given law. Because of the restricted sense of shear along the glide direction in the composition plane, information on the principal stress direction may be obtained from these measurements.

In albite twinning (Fig. 2), (010) is the twin plane and the twin operation is a reflection on (010). This corresponds to a rotation of 180° about axis $\mathbf{b}^*$, perpendicular to (010). In albite twinning, the twin plane and the composition plane are the same. The angle between **b** and $\mathbf{b}^*$ is the obliquity, $\varphi = \mathbf{b} \wedge \mathbf{b}^*$, typically about 4° in ordered natural plagioclases. In Pericline twinning (Fig. 2), **b** is the twin axis and the composition plane is the so-called rhombic section (Smith and Brown, 1988).

Table 1
Definitions of plagioclase glide twinning[a]

| Element | Symbol | Albite law | Pericline law |
|---|---|---|---|
| Glide plane | K1 | (010) | rhombic section |
| 2nd circular section | K2 | $\mathbf{s}^*$ | $\mathbf{b}^*$ |
| Glide direction | N1 | $\mathbf{s} = [U0W]$ | $\mathbf{b} = [010]$ |
| Angle of shear | $\psi$ | $2\varphi$ | $2\varphi$ |
| Shear | $\gamma$ | $2\tan(\psi/2) = 2\tan(\varphi)$ | $2\tan(\psi/2) = 2\tan(\varphi)$ |

[a] $\mathbf{s}^*$ is known as the rhombic section; both $\mathbf{s}^*$ and $\mathbf{s}$ have irrational indices. For a composition typical of our samples $An_{37.4}$, obliquity $\varphi = \mathbf{b} \wedge \mathbf{b}^* = 3.8575$, $\psi = 7.7150$ and $\gamma = 0.1348$.

Albite and pericline twins are the only twins which can strictly form by gliding (Smith and Brown, 1988). The glide directions lie in the composition plane, (010) or in the rhombic section, respectively; the angular deviation in both cases being $2\varphi$ ($\varphi$ is the obliquity $\varphi = \mathbf{b} \wedge \mathbf{b}^* = \mathbf{s} \wedge \mathbf{s}^*$). For pericline twins the glide direction is $\mathbf{b}$ (Fig. 2), whereas for albite twins the glide direction, $\mathbf{s}$, has irrational indices, [u0w]. The two slip planes and the two slip lines are conjugate to each other (Fig. 2). A summary of the twin gliding elements of plagioclase is given in Table 1. The orientation of the principal stress directions associated with mechanical twinning can be most easily specified with the introduction of the rhombic line unit vector ($\mathbf{r}$), which is perpendicular to $\mathbf{b} = [010]$, $\mathbf{b}^* = \perp(010)$, $\mathbf{s} = [U0W]$, and the rhombic section $\mathbf{s}^* = \perp(H0L)$. The rhombic line unit vector in the positive sense ($+\mathbf{r}$) is given by

$$+\mathbf{r} = (\mathbf{b} \times \mathbf{b}^*)/|\mathbf{b} \times \mathbf{b}^*| = (\mathbf{s}^* \times \mathbf{s})/|\mathbf{s}^* \times \mathbf{s}| \quad (1)$$

where all vectors are taken in the positive sense and $+\mathbf{r}$ makes angle ($\alpha$) with $+\mathbf{a} = [100]$ in the (010) plane (Fig. 2). The rhombic line can be used to define the irrational indices of $\mathbf{s}^*$ and $\mathbf{s}$ as

$$\mathbf{s}^* = +\mathbf{r} \times \mathbf{b} = (\mathbf{b} \times \mathbf{b}^*) \times \mathbf{b} \quad (2)$$

$$\mathbf{s} = +\mathbf{r} \times \mathbf{b}^* = (\mathbf{b} \times \mathbf{b}^*) \times \mathbf{b}^* \quad (3)$$

The $+\mathbf{r}$ is parallel to the intersection of the conjugate albite and pericline glide planes. The maximum resolved shear stress is produced for the positive sense for twinning only if the maximum compressive stress direction ($\sigma_1$) lies at the acute bisectrix of $+\mathbf{b}$ and $-\mathbf{s}$, the intermediate stress direction ($\sigma_2$) is parallel to the rhombic line ($+\mathbf{r}$) and the extension stress direction ($\sigma_3$) is parallel to ($\sigma_1 \times \sigma_2$) which is between $+\mathbf{b}$ and $+\mathbf{s}$. Using these crystallographic relationships we can define the orientation of the stress axes with respect to the plagioclase crystal axes for any composition, and assign irrational [uvw] indices for each stress axis.

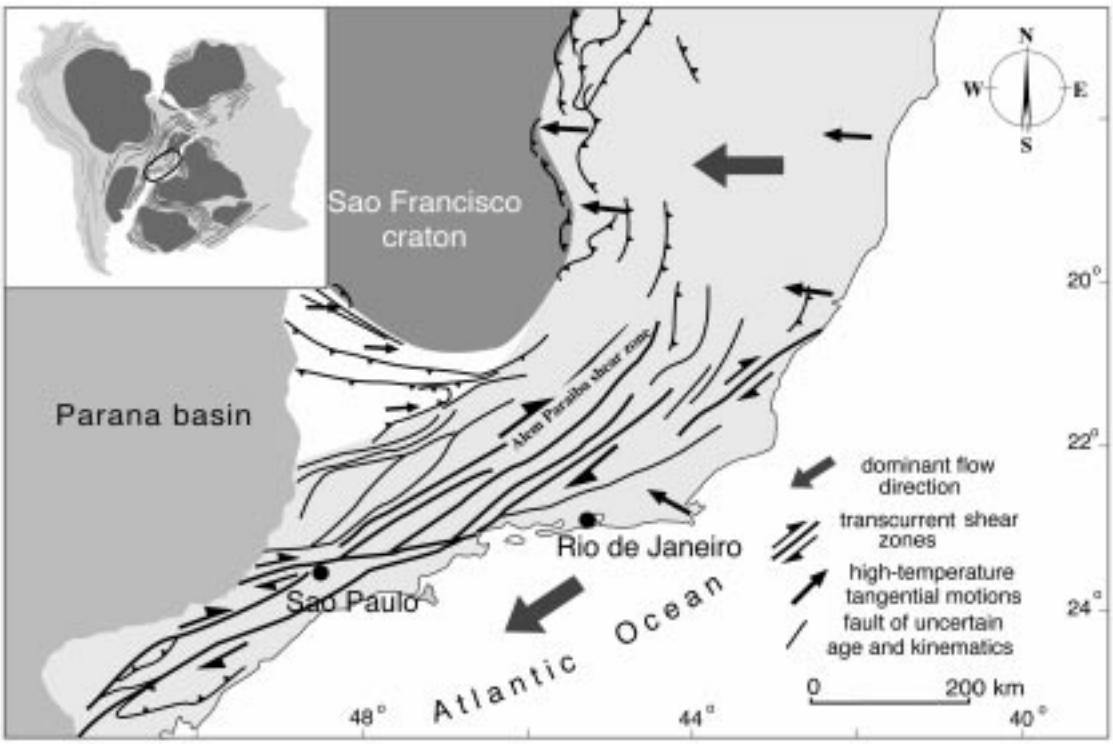


Fig. 3. Schematic map of the southern portion of Ribeira–Araçuaí belt showing Além Paraíba shear zone and the dominant kinematics (modified from Vauchez et al., 1994).

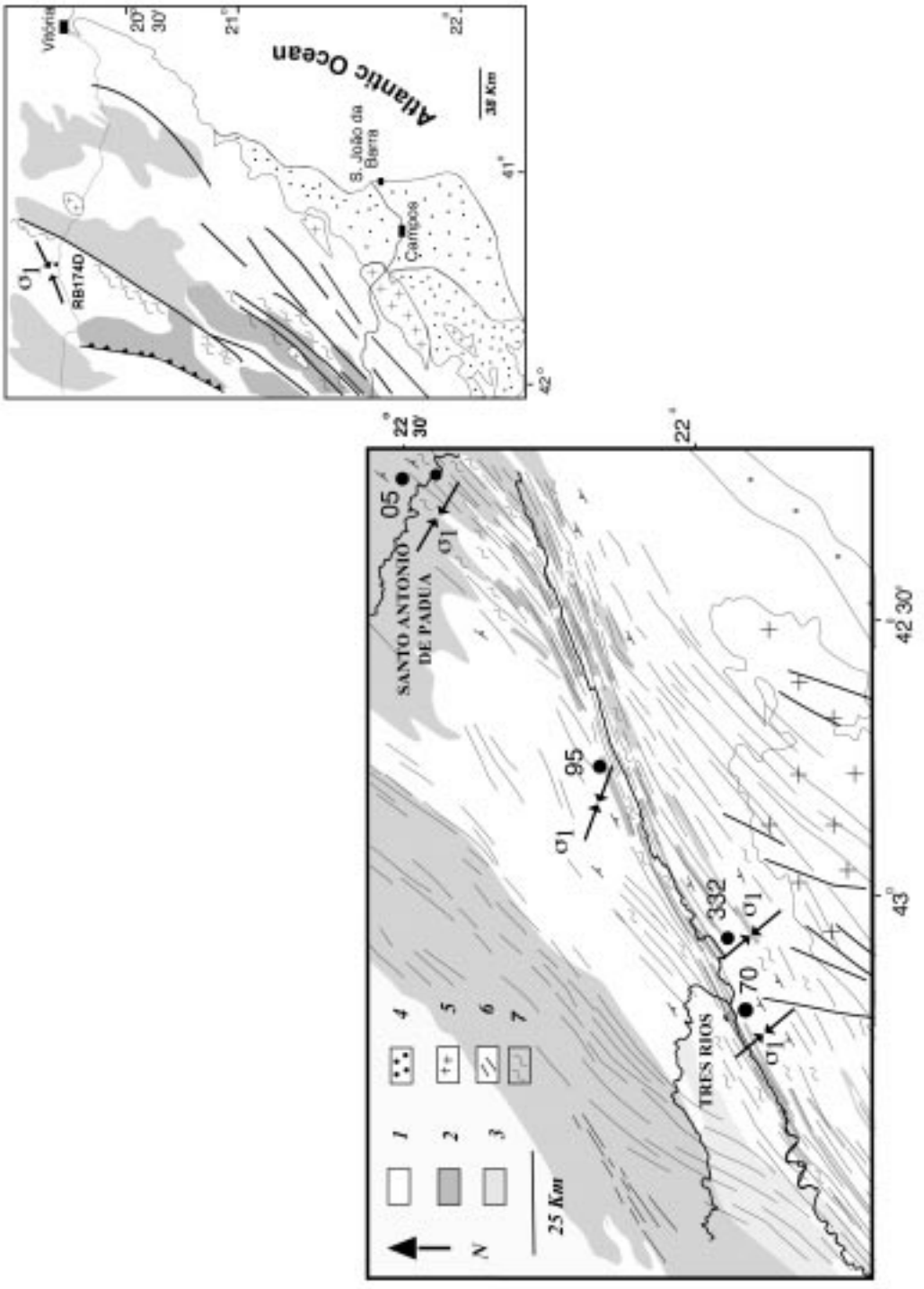


Fig. 4. Schematic geologic map from Além Paraíba shear zone and the localization of the studied samples and the stress directions determined from plagioclase fabrics. (1) Polycyclic basement. (2) Juiz de Fora Compex. (3) Enderbite. (4) Kinzigite. (5) Syntectonic granites. (6) Paraiba do Sul Complex. (7) Mylonitic rocks.

## 3. Measurement procedure

In order to determine the principal stress axes orientations, determination of plagioclase lattice-preferred orientation was performed using U-stage measurements. Crystallographic axes orientations were inferred with the aid of an interactive computer program developed by Benn and Mainprice (1989), which allows complete crystallographic determination of the positive and negative crystal axes proposed by Wenk et al. (1986) and based on the optical data compiled for the plagioclase solid solution series by Burri et al. (1967).

An electron microprobe (JEOL JXA-8600) was used to obtain the composition of the plagioclases from the five samples used in this study.

## 4. Geological setting

The Ribeira belt (Fig. 3) extends over more than 1500 km along the southeast coast of Brazil. This belt (see review in Trompette, 1994) was formed along the eastern and southeastern margins of the São Francisco craton, in response to the convergence between the São Francisco and Congo cratons, during the Brasiliano (Neoproterozoic) orogeny (Vauchez et al., 1994).

The Ribeira belt consists of: (1) a cratonic basement (Complexo Juiz de Fora) which records granulite facies metamorphism at $2220 \pm 27$ Ma (Söllner et al., 1991); (2) a well-developed Paleoproterozoic metasedimentary sequence (Complexo Paraíba do Sul) involving kinzigites, garnet–biotite–plagioclase gneisses, migmatites and granulite gneisses from the Transamazonian tectonic cycle (2000 Ma). These units have been intensively reworked by tectonic, magmatic and metamorphic processes during the last important orogenic event (Brasiliano orogeny) in this region.

The northern part of the belt trends almost north–south, bordering the São Francisco craton eastward. Kinematic data collected in this area by various authors consistently indicate westward transport towards the São Francisco craton (Pedrosa-Soares et al., 1992; Trompette et al., 1992). Approaching the southern edge of the craton from the north, the deformation pattern changes progressively. The structural trend rotates from north–south to northeast, and narrow ductile strike-slip faults, parallel to the belt northward, progressively widen and merge southward, forming several mylonite zones ~10 km thick oriented NE–SW. The Além Paraíba shear zone is one of these mylonite zones (Fig. 3). It is a continental-scale, strike-slip fault occuring in the north-central portion of Rio de Janeiro state. Deformation in the Além Paraíba shear zone is attributed to the late stages of collision between the São Francisco and Congo cratons around 570–600 Ma ago (Vauchez et al., 1994).

## 5. Geological contexts of the samples

The rocks used in this study are from the Juiz de Fora and Paraíba do Sul Complexes which are granulites of norite composition, garnet–biotite–plagioclase gneisses, amphibolites, pyroxenes–plagioclase gneisses and some biotite-rich migmatites. From the apparently stable parageneses and homogeneous element distributions between co-existing phases as inferred from microprobe analysis, it has been determined that the temperature of the first metamorphic event $M_1$ ($D_1$-deformation) varies between 700°C (hornblende–garnet) and 710–750°C (garnet–biotite) in the southern and northern areas, respectively, with pressure varying between 500 and 560 MPa (garnet–plagioclase–biotite–quartz–sillimanite). The second metamorphic event $M_2$ ($D_2$ deformation) temperatures vary between 680 and 690°C (garnet–biotite) with pressures increasing from 590 to 700 MPa northward (Porcher et al., 1995; Fernandes et al., 1996).

We have studied five samples, which have been collected from two different tectonic contexts. The samples RB70, RB332, and RB95 were deformed under granulite facies conditions in the Além Paraíba shear zone (Fig. 4). In this structural domain, the predominant NE–SW structures overprint a flat-lying fabric ($D_1$) whose kinematic indicators suggest overthrusting towards WNW. In the southern domain, these rocks are strongly foliated (N 055/ vertical) with a horizontal stretching lineation. Most of the kinematic indicators ($S/C$ fabrics, asymmetric porphyroclasts ($\delta$ and $\sigma$ types), mica fish and lattice-preferred orientations of quartz and plagioclase) are consistent with a dextral movement of shear. These specimens are from a mylonitic granodiorite, with plagioclase (anorthite; $An_{25-38}$) as the predominant mineral (55–60%) and quartz (20–25%). The only common mafic mineral is biotite (~13%) with accessory minerals such as garnets, zircon and carbonates in amounts smaller than 5% of the rock volume.

The sample RB05 is a mangerite gneiss composed predominantly of plagioclase ($An_{38}$–$An_{40}$) (~60%), quartz (~20%) and pyroxenes (~3%). It is a foliated rock from the northern part of the Além Paraíba shear zone, where the deformation pattern begins progressively to change from a transpression to compression regime and the foliation trend rotates from northeast to north (Fig. 4). In this region the foliation strikes N35–38° and dips 45–50° southeastward.

These rocks were deformed under granulite facies conditions. Hypersthene, a mineral typical of the gran-

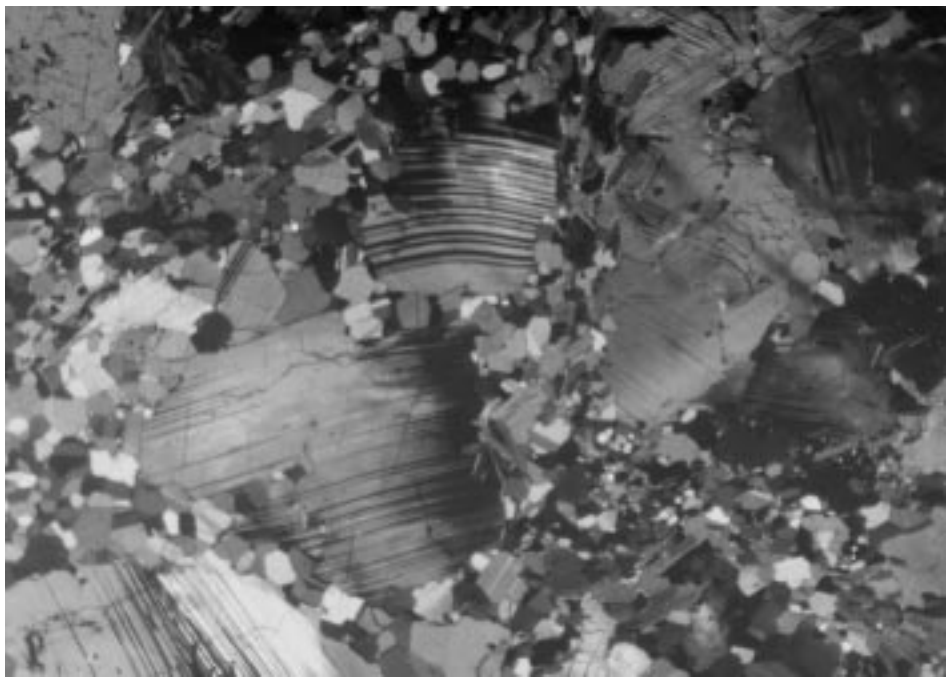

Fig. 5. Sheared gneisses from Além Paraíba fault with bent plagioclase porphyroclasts (10×).

ulite facies, shows no retrogression and is involved in the foliation plane.

Sample RB174 is a norite gneiss from the northern part of the Ribeira belt where a westward (overthrusting) transport prevails (Fig. 4). This rock is composed predominantly of plagioclase ($An_{55}$–$An_{57}$) (~80%), pyroxenes (~15%) and quartz (~3%). In this region the foliation strikes north–south and dips gently, 25–35°, eastward, and the lineation is almost east–west.

## 6. Microstructures and fabrics of the plagioclase

The mylonitic gneisses (RB70, RB95 and RB332) of the Além Paraíba shear zone show well-developed

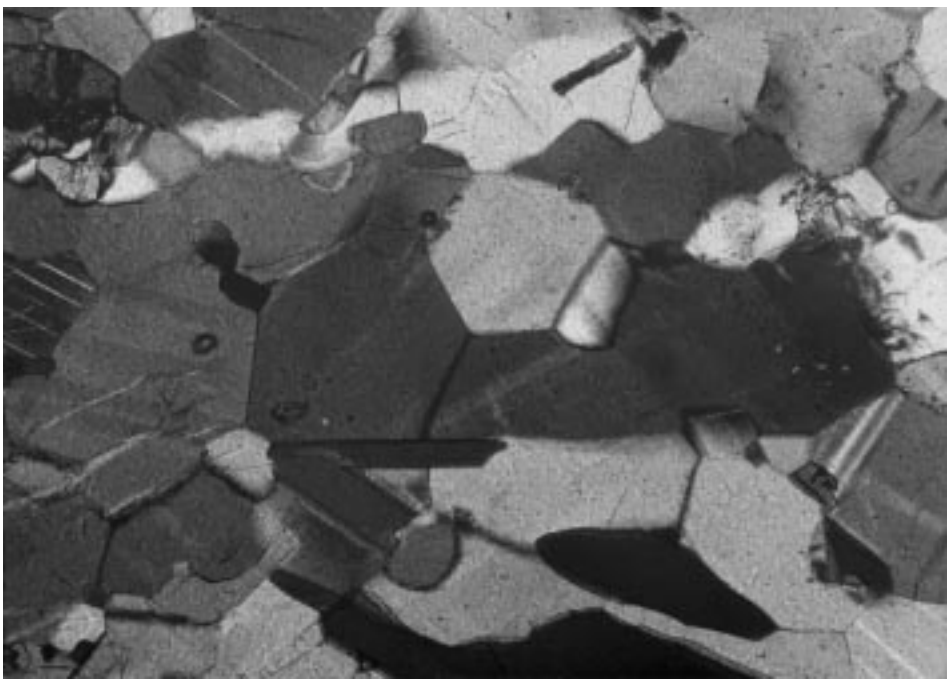

Fig. 6. Recrystallized plagioclase grains with polygonal shapes. Straight grain boundary configurations meet at 120° triple junctions (20×).

Table 2
Plagioclase twin frequency

| Specimen | Thin section | Only albite (%) | Only pericline (%) | Albite and pericline (%) | Total number of grains |
|---|---|---|---|---|---|
| RB70 | XZ | 78.57 | 18.09 | 3.3 | 210 |
| | YZ | 86.11 | 11.11 | 2.7 | 108 |
| | XY | 87.5 | 10.0 | 2.5 | 040 |
| RB332 | XZ | 84.37 | 10.62 | 5.0 | 160 |
| RB95 | XZ | 85.45 | 14.54 | | 110 |
| RB05 | XZ | 87.30 | 11.33 | 1.33 | 150 |
| RB174 | XZ | 71.78 | 21.15 | 7.05 | 156 |
| | YZ | 76.65 | 12.67 | 10.67 | 150 |

recrystallized aggregates of plagioclase and quartz with a small amount (less than 15%) of porphyroclasts. Both quartz and plagioclase porphyroclasts generally exhibit undulose extinction associated with the development of subgrains and bending of polysynthetic twins in plagioclase (Fig. 5).

Dynamic recrystallization in each of the three samples is characterized by a bimodal crystal size distribution and the recrystallized grains (smaller grains or neoblasts) show a similar composition to the respective 'porphyroclast' grains. Grain boundary migration and subgrain rotation are the principal processes of recrystallization in these samples.

Deformation microstructures (undulose extinction and deformation twins are the most common) are observed within both the larger plagioclase grains and the smaller recrystallized plagioclase grains. The porphyroclasts are generally more strongly deformed than the recrystallized grains; most of these grains are just slightly deformed. The deformation twins (albite and pericline laws) generally terminate at grain boundaries, to a fine point within the grains.

Sample RB05 is nearly completely recrystallized (quartz and plagioclase). The recrystallization process is predominantly by grain boundary migration and probably would have been driven by surface energy, whereby most of the grain boundaries are straight and tend to intersect at 120° (Fig. 6). Some grains of plagioclase and quartz are almost strain free, as indicated by the even extinction of individual grains and relatively straight grain boundaries. Progressive recrystallization during the late stage of the deformation, and grain boundary migration can lead to larger grains with straight boundaries and 120° intersections (e.g. Davis and Reynolds, 1996).

Sample RB174 displays little evidence of recrystallization of the plagioclase grains but most of them show mechanical twins and weak undulose extinction.

Therefore, three different situations may be considered for the lattice-preferred orientation studies: (i) the samples (RB70, RB332 and RB95) for which the predominant recrystallization processes are grain boundary migration and subgrain rotation; (ii) a sample (RB05) which has grain boundary migration as the main recrystallization process followed by annealing during the late stages of the recrystallization; and (iii) a sample (RB174) with little evidence of recrystallization.

Plagioclase lattice-preferred orientation (LPO) was obtained from measurements of the optical indicatrix plus two different crystallographic planes (cleavages or twins). In order to have a statistically meaningful

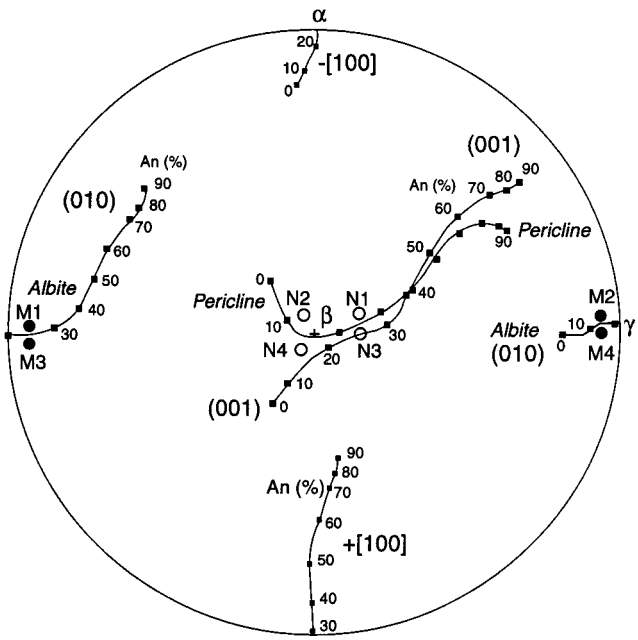


Fig. 7. Plagioclase determinative diagram from Burri. Migration curves give orientations of planar elements with respect to three optical axes ($\alpha, \beta\, \gamma$). Black circles $M_1$, $M_2$, $M_3$ and $M_4$, and open circles $N_1$, $N_2$, $N_3$ and $N_4$ represent four possible orientations for albite and pericline twin planes or for (010) and (001), respectively, with respect to $\alpha$, $\beta$ and $\gamma$ directions in a plagioclase $An_{25}$. For anorthite contents $An_{10}$–$An_{35}$, the angular distance between $M_1$ and $M_3$, $M_2$ and $M_4$, $N_1$ and $N_3$ and $N_2$ and $N_4$ is too small ($\leq 5°$) to be discerned by U-stage measurement, causing ambiguity in the determination of complete crystallographic orientations (from Ji et al., 1994).

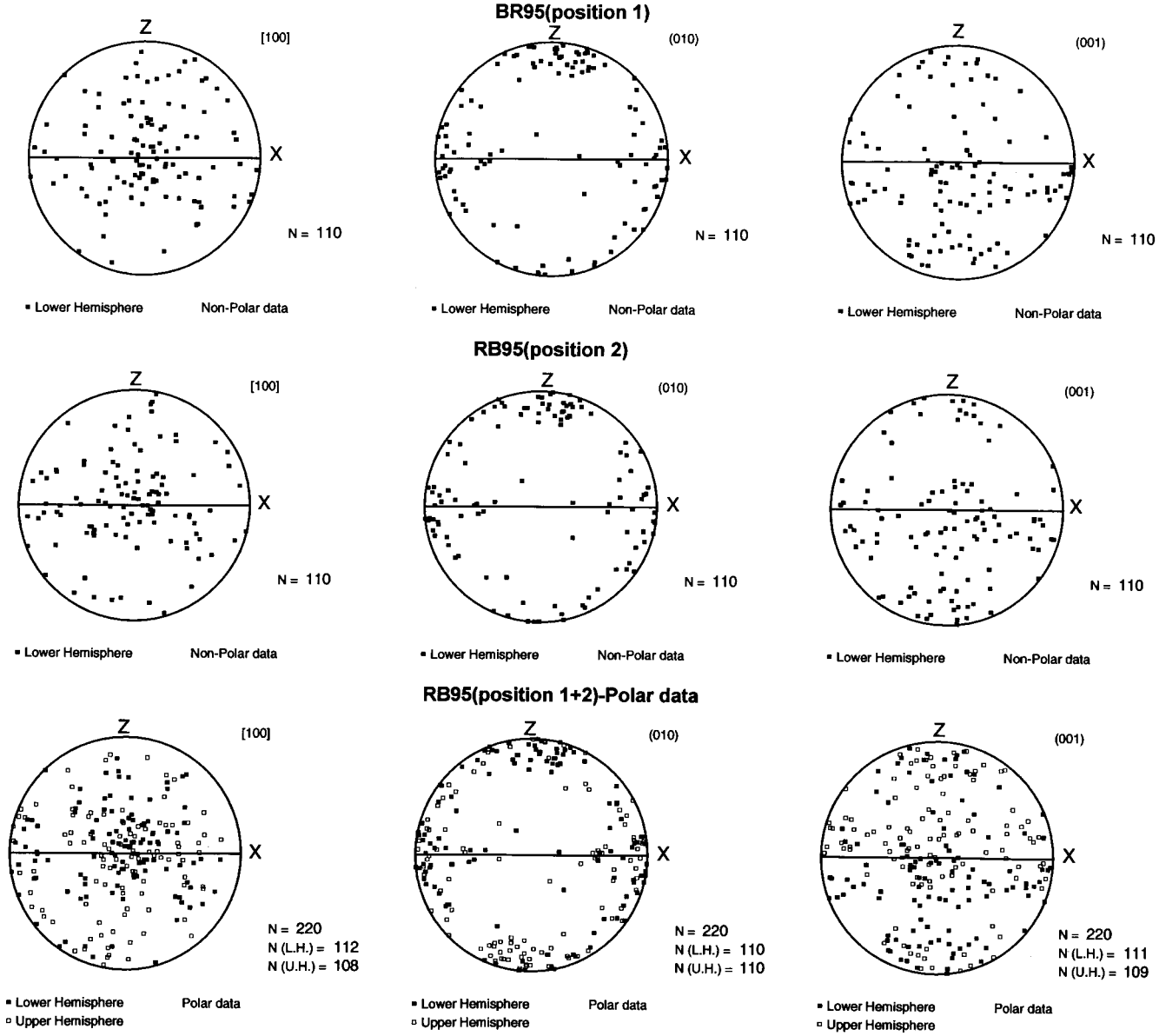


Fig. 8. Crystallographic axes orientation diagrams for the two possible positions using non-polar data, and using polar data for positions 1 + 2 (sample RB95).

description of the LPO, the measurements were taken in three perpendicular sections (XZ, YZ and XY) for sample RB70 and in two perpendicular sections (XZ and YZ) for sample RB174. For the other samples (RB05, RB95 and RB332) measurements were performed only for the XZ section. The data from the YZ and XY sections were rotated to the XZ plane before analysis and interpretation. These sections have a significant number of grains with at least one twinning plane (albite or pericline). The albite twin prevails in all sections, pericline twins are less abundant, and grains with both twins are uncommon (Table 2).

The anorthite content of plagioclase in sample RB95 is within the range $An_{20–30}$. Consequently, measuring only the (010) cleavage or the compositional plane of the albite twin is not enough to permit unambiguous determination of the plagioclase orientation (Kruhl, 1987b; Ji et al., 1994). There are four possible orientations for the measured plane to be plotted onto the plagioclase determinative diagram (Fig. 7). The black circles $M_1$, $M_2$, $M_3$ and $M_4$, and open circles $N_1$, $N_2$, $N_3$ and $N_4$ represent four possible orientations for measured albite and pericline twin planes or for (010) and (001), respectively, with respect to $\alpha$, $\beta$, $\gamma$ directions in a plagioclase $An_{25}$. We know the anorthite contents of this sample ($An_{25}$), so there are only two

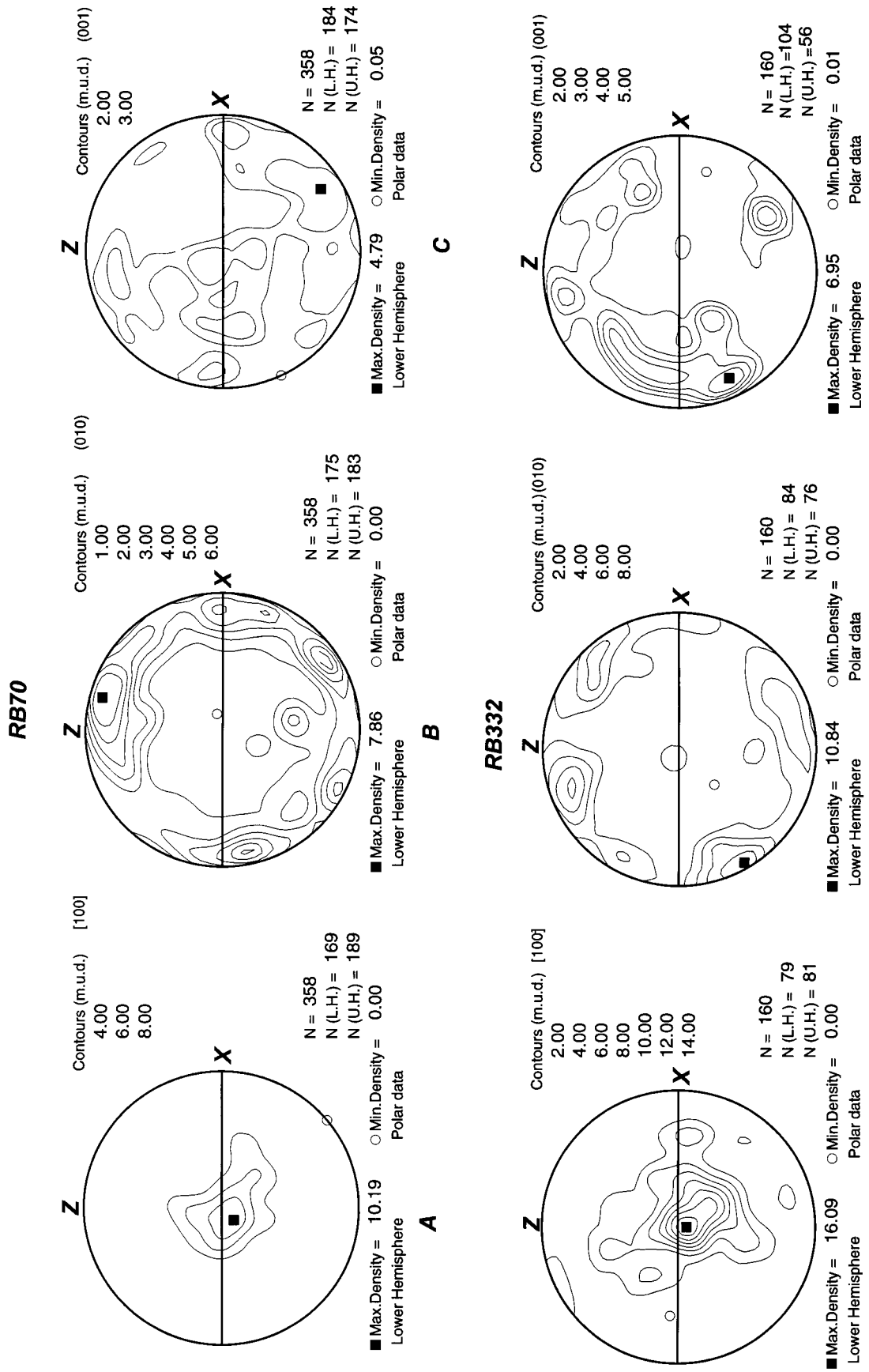


Fig. 9. Preferred orientation of plagioclase crystallographic axes in the gneiss mylonite from the Além Paraíba shear zone (samples RB70A and RB332).

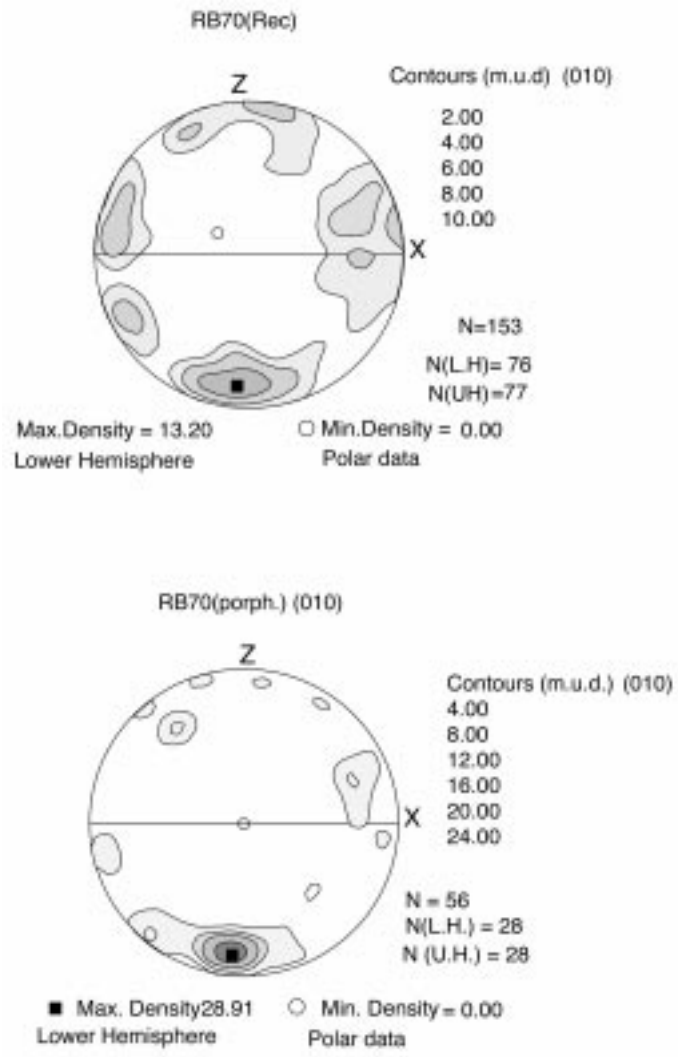


Fig. 10. Preferred orientation of (010) planes from porphyroclast and recrystallized plagioclases (sample RB70).

possible crystallographic orientations that can fit the angular constraints for these plagioclases; they are $M_1$ and $M_3$, if the measured plane was an albite, or (010), or $N_1$ and $N_3$ if the measured plane was a pericline or (001) (Fig. 7). As we could not determine the correct position we constructed the crystallographic axes orientation diagrams for the two possible positions and we realized that non-polar data diagrams were very similar (Fig. 8) and that there was no difference regarding kinematic aspects.

The preferred orientations of (010), (001) and *a* (samples RB70 and RB332) are shown in Fig. 9. The LPO strength is high with [100] axes occupying the centre of the diagram and ⊥(010) displaying two maxima, the principal one almost perpendicular to the foliation and a secondary maximum subparallel to the stretching lineation (Fig. 9B). In spite of the weak asymmetry of (010) with respect to the foliation and lineation in the sample RB70, it is consistent with a dextral shear movement. The ⊥(001) planes orientation define a diffuse girdle, with a maximum at 35°/120° (dip/direction). LPO for sample RB332 is similar, except for the ⊥(010) orientation pattern whose maximum is at 5°/240°, and there is a striking asymmetry in agreement with a dextral shear movement (Fig. 9E). A secondary maximum close to the Z-axis can also be observed in sample RB332. The ⊥(001) orientation pattern is always difficult to interpret but we can record a maximum at 15°/245°.

The preferred orientation patterns of the porphyroclasts and recrystallized plagioclases (sample RB70) have their (010) planes subparallel to the foliation plane (XY plane; Fig. 10). This means that the pattern of preferred orientation of the neoblasts is similar to that of the porphyroclasts. The similar orientation for both suggests that the neoblasts were recrystallized from a host favorably oriented for easy glide, because if the neoblasts had been developed from a host unsuitably oriented for easy glide, the grains would be in a different orientation pattern to their host (Ji and Mainprice, 1990).

The crystallographic orientation patterns of the other samples (RB95 and RB5; Fig. 11) are similar, the *a* direction is preferentially oriented subparallel to Y-axis. Most grains have the ⊥(010) planes close to the Z-axis of finite strain (Fig. 11B and E). The orientation pattern of the (001) poles is always more complex and defines diffuse girdles, one in the foliation plane (XY) and another subparallel to the YZ plane (Fig. 11F and C, respectively).

The fabric of sample RB174 (weakly recrystallized) shows a preferred orientation with [100] axes in the foliation plane (XY) and maximum density at 55°/080° (Fig. 12). It is different from the other samples where the [100] axes are parallel to Y. The (010) poles are at maximum subparallel to Z-axes (5°/185°). We have observed a similar position for the other samples. The absence or very weak asymmetry of the (010) poles relative to the foliation does not allow deduction of the shear sense in this sample. The poles of the (001) planes show a maximum density at 20°/000°.

## 7. Stress direction determination

In order to determine the stress directions from plagioclase fabrics, these LPO data were plotted for each studied sample taking all the geometric elements of mechanical albite and pericline twins into account. This allows determination of the compression axis for each grain and, statistically, the best orientation for $\sigma_1$ (Fig. 1).

The integrated stress directions data for the sample RB70 are shown in Fig. 13. The statistical diagrams

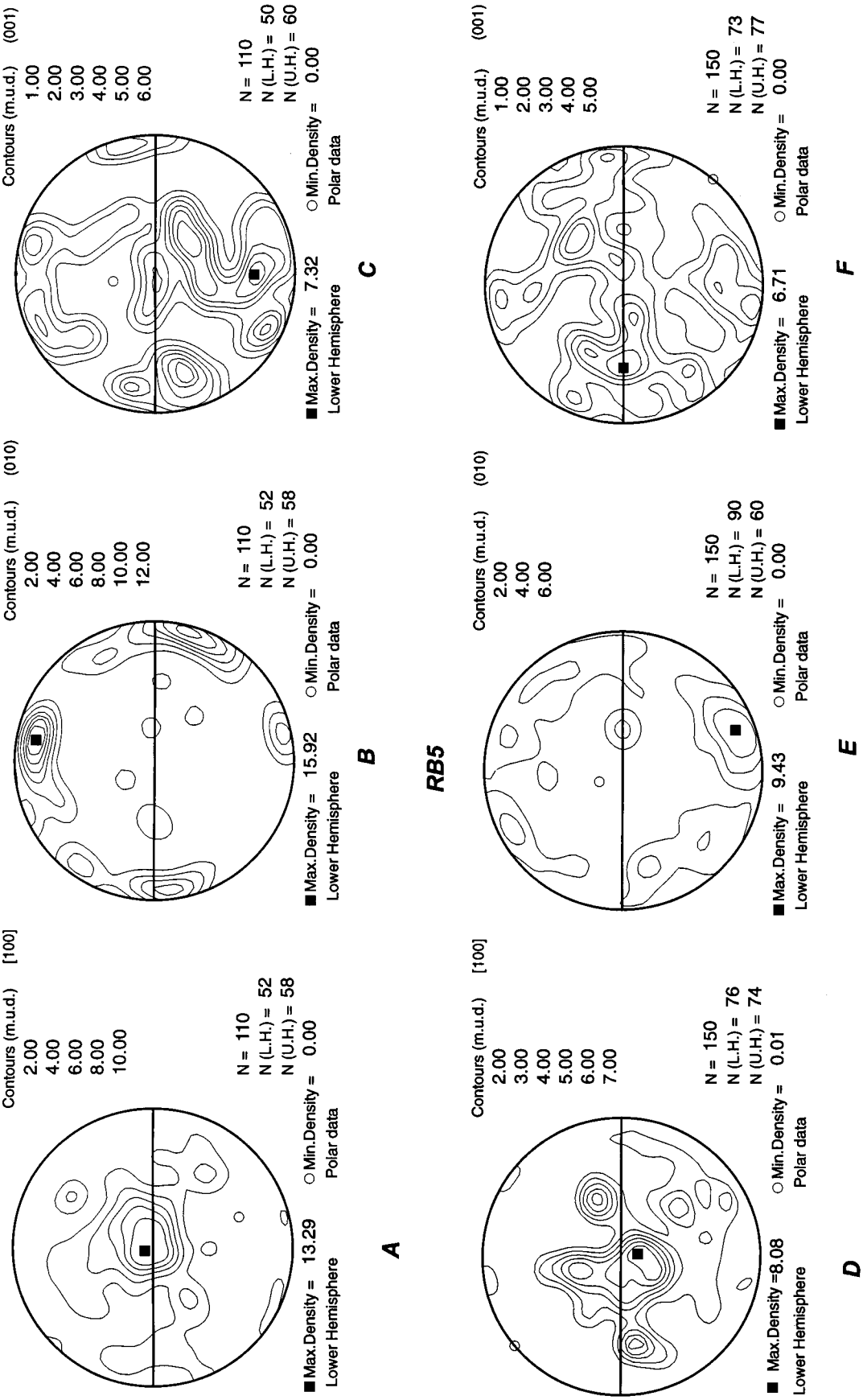


Fig. 11. Preferred orientation of plagioclase crystallographic axes in mylonites from the Além Paraíba shear zone (samples RB95 and RB5).

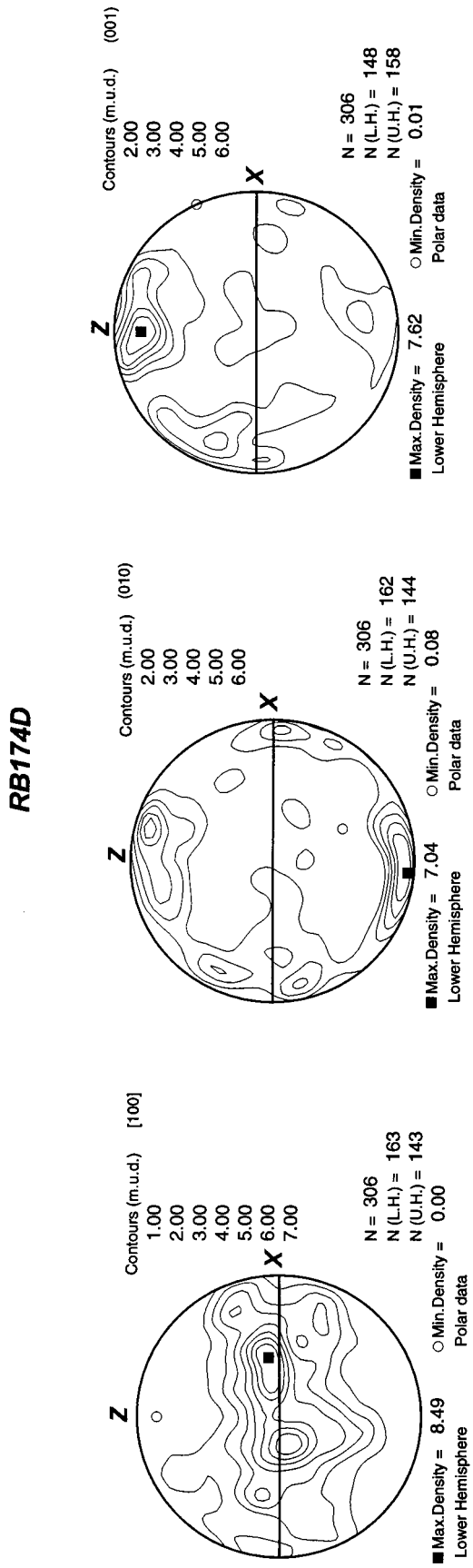


Fig. 12. Preferred orientation of plagioclase crystallographic axes in the norite gneiss from Juiz de Fora Complex (northern portion of Ribeira belt; sample RB174D).

show maximum values for $\sigma_1$, $\sigma_2$ and $\sigma_3$ at 5°/185°, 85°/250° and 2°/100°, respectively. The maximum compressive stress is subparallel to the foliation pole, the intermediate is parallel to Y and the minimum is parallel to stretching lineation X. The albite twin direction [U0W] (Fig. 13D) has a complex distribution pattern but displays maximum density subparallel to $\sigma_1$. The albite plane orientations (Fig. 13E) show a distribution similar to the (010) planes (Fig. 9B). The pericline twin planes +(hol) and directions +[010] show a maximum at X and Z, respectively.

The stress directions determined for sample RB332 are similar to the latter ones but there is a weak asymmetry of $\sigma_1$ (15°/115°) (Fig. 14A) relative to the foliation plane. The maximum density of albite twin direction is 15°/115°, subparallel to the maximum density of albite and pericline planes (Fig. 14E, F and G). The intermediate and minimum stresses show a maximum statistical distribution at 85°/205° and 15°/60°, respectively.

Because of the plagioclase composition ($An_{30}$) for sample RB95, we have performed the statistical treatment regarding the only two different possible positions that can fit the crystallographic orientations and angular constraints for these plagioclases (Fig. 8). Fig. 15 shows the stress orientations regarding positions 1 and 2 separately and the diagrams with both data (Fig. 15G, H and I). The maximum, intermediate and minimum stress directions are remarkably consistent for all diagrams ($\sigma_1 = 5°/145°$; $\sigma_2$ = subvertical and $\sigma_3 = 10°/50°$). This observation implies that no matter the selected position, the stress directions deduced from LPO analysis are similar (Fig. 15). The stress pattern is consistent with a non-coaxial deformation and a dextral shear sense. However, the albite directions +[U0W] (Fig. 16A and E) and pericline planes (Fig. 16D and H) have a different orientation regarding the distinct positions.

The analysis performed for sample RB5 has led to the reconstruction of the paleostress field where maximum density orientation of $\sigma_1$ is subparallel to foliation pole (Z), $\sigma_2$ is parallel to the Y-axis and $\sigma_3$ is subparallel the stretching lineation (X) (Fig. 17A, B and C). The albite direction has a maximum density close to the diagram center (Y) (Fig. 17D) and albite plane and pericline directions show similar patterns with a maximum at 10°/160° (Fig. 17F and E).

The sample RB174, from another tectonic context outside the transcurrent shear zone yielded the maximum compressive stress direction ($\sigma_1$) at 5°/155°; the intermediate stress ($\sigma_2$) subvertical, and the minimum stress ($\sigma_3$) with the highest density at 20°/60° (Fig. 18A, B and C). In this region the foliation plane strikes north–south and dips gently 30° eastward, and consequently the stress directions with regard to the foliation plane (in the field, not at the Universal stage

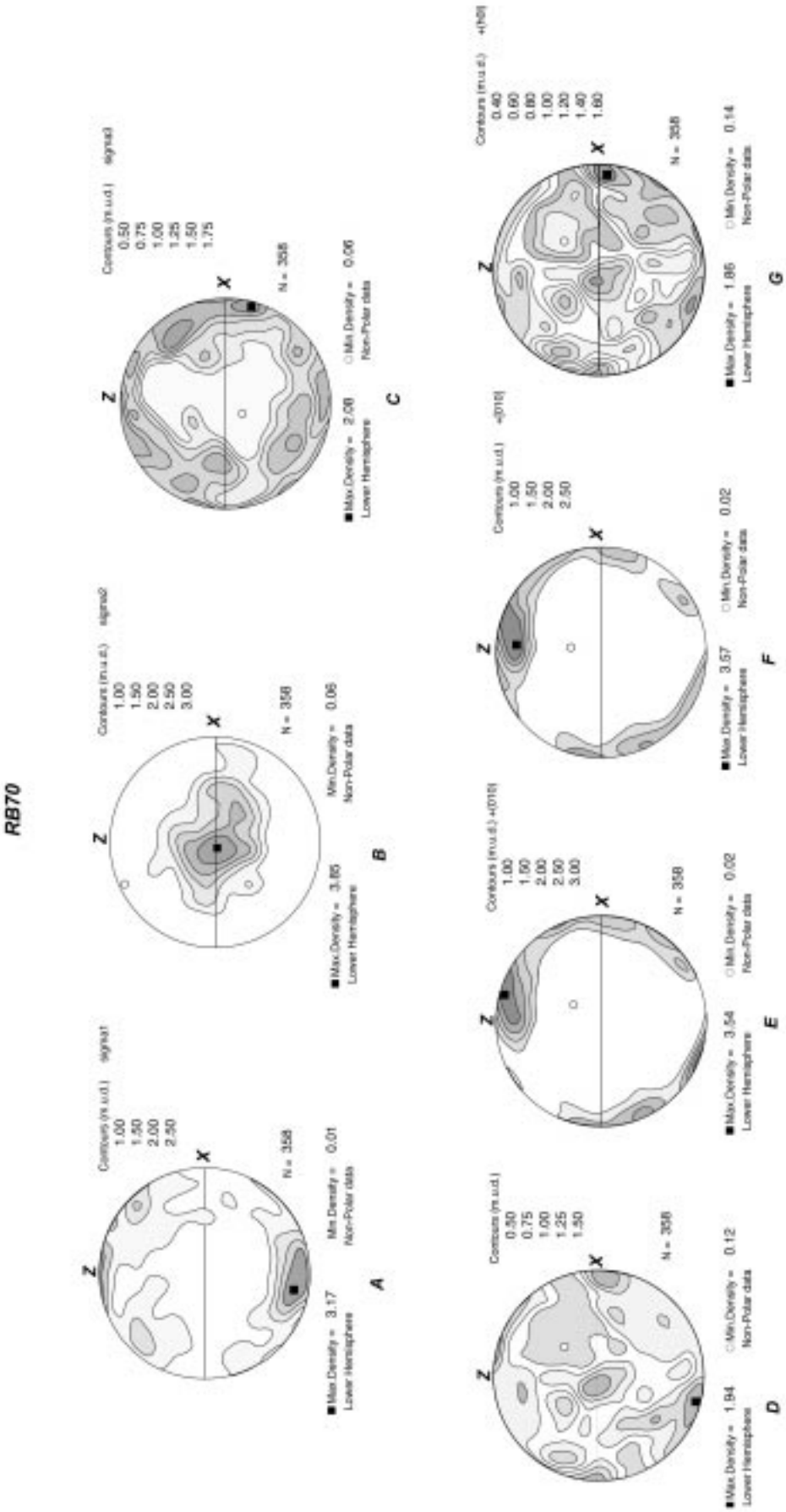


Fig. 13. Statistical distribution diagrams of the stress directions (A, B and C), albite and pericline directions (D and F), and albite and pericline planes (E and G) (sample RB70).

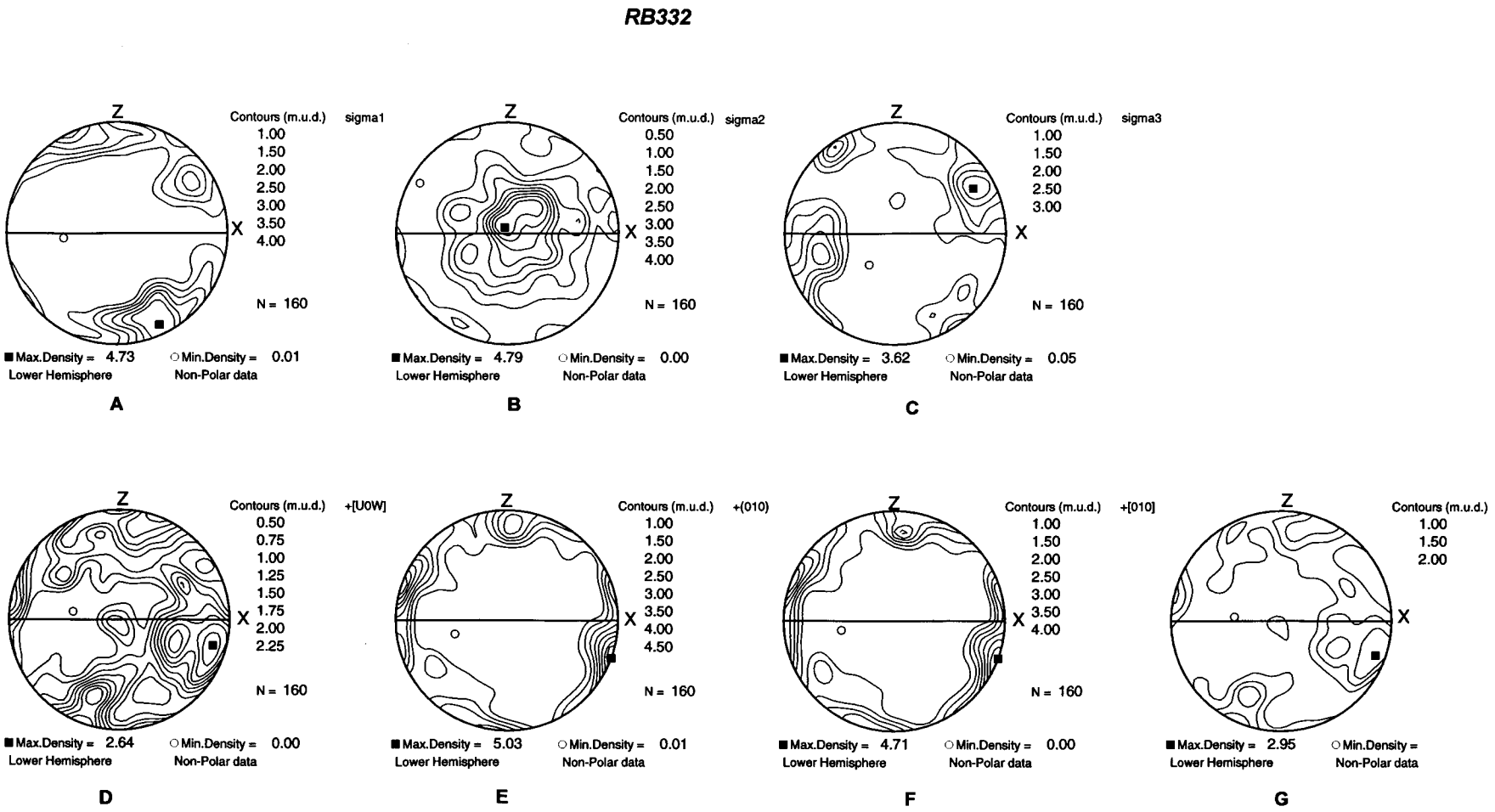


Fig. 14. Isofrequency diagrams for stress directions ($\sigma_1$, $\sigma_2$, $\sigma_3$) relative to sample RB332 (A, B and C, respectively). Albite and pericline directions (D and F) and albite and pericline planes (E and G).

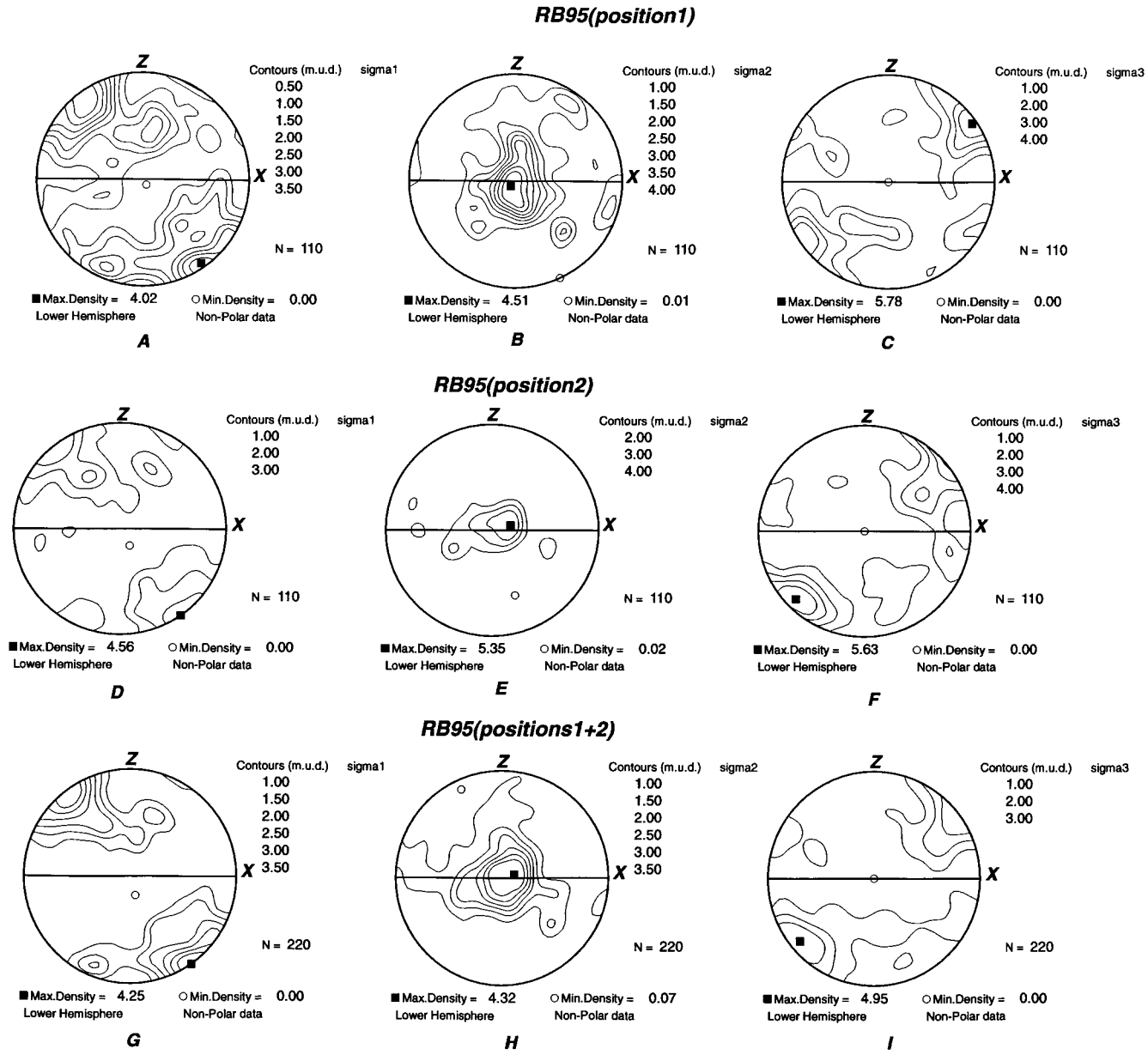


Fig. 15. Isofrequency diagrams for stress directions ($\sigma_1$, $\sigma_2$, $\sigma_3$) relative to sample RB95. The positions 1 and 2 (A, B, C and D, E, F, respectively) show no different stress orientations.

plane) are 46°/228° ($\sigma_1$); 26°/115° ($\sigma_2$) and 36°/006° ($\sigma_3$).

The five samples which have been studied to determine stress directions have yielded consistent results. The statistical distribution of $\sigma_1$ directions shows a maximum not far from the foliation pole, sometimes consistent with a dextral shear movement (RB95, RB332 and RB174) (Figs. 14, 15 and 18); and, sometimes coherent with a coaxial deformation (Figs. 13 and 17). The intermediate and minimum stresses are always subparallel to Y and X, respectively.

## 8. Discussion and conclusions

### *8.1. Lattice-preferred orientation (LPO) and recrystallization*

The orientation patterns of the distinct crystallographic axes and planes show similarities and small differences:

1. the *a* direction forms a pronounced maximum at Y for all the samples.

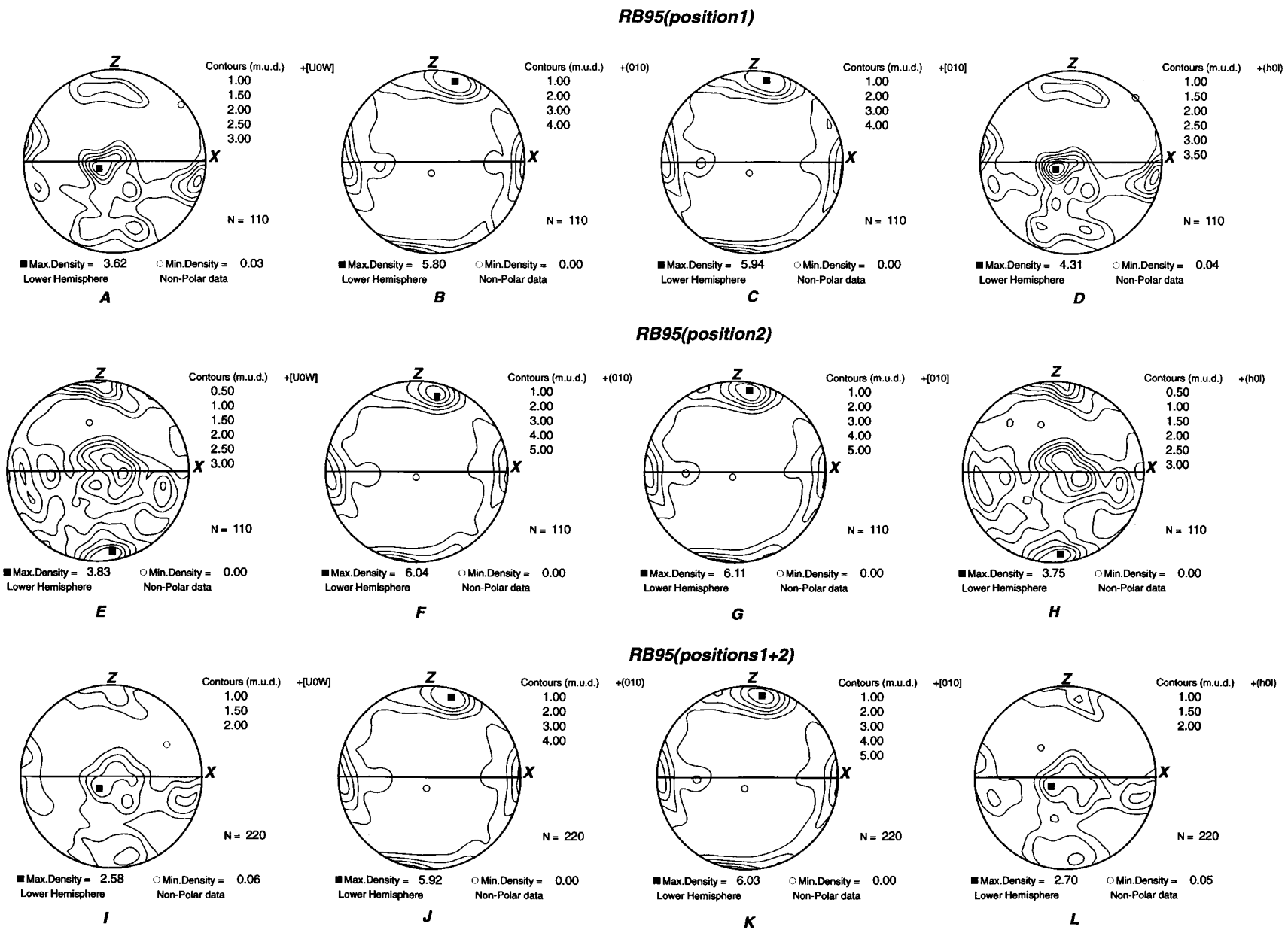


Fig. 16. Albite and pericline directions (A and C) and albite and pericline planes (B and D) for position 1. Albite and pericline directions (E and G) and albite and pericline planes (F and H) for position 2. The diagrams I and K are from albite and pericline directions, whilst J and L are from albite and pericline planes, considering data from both positions.

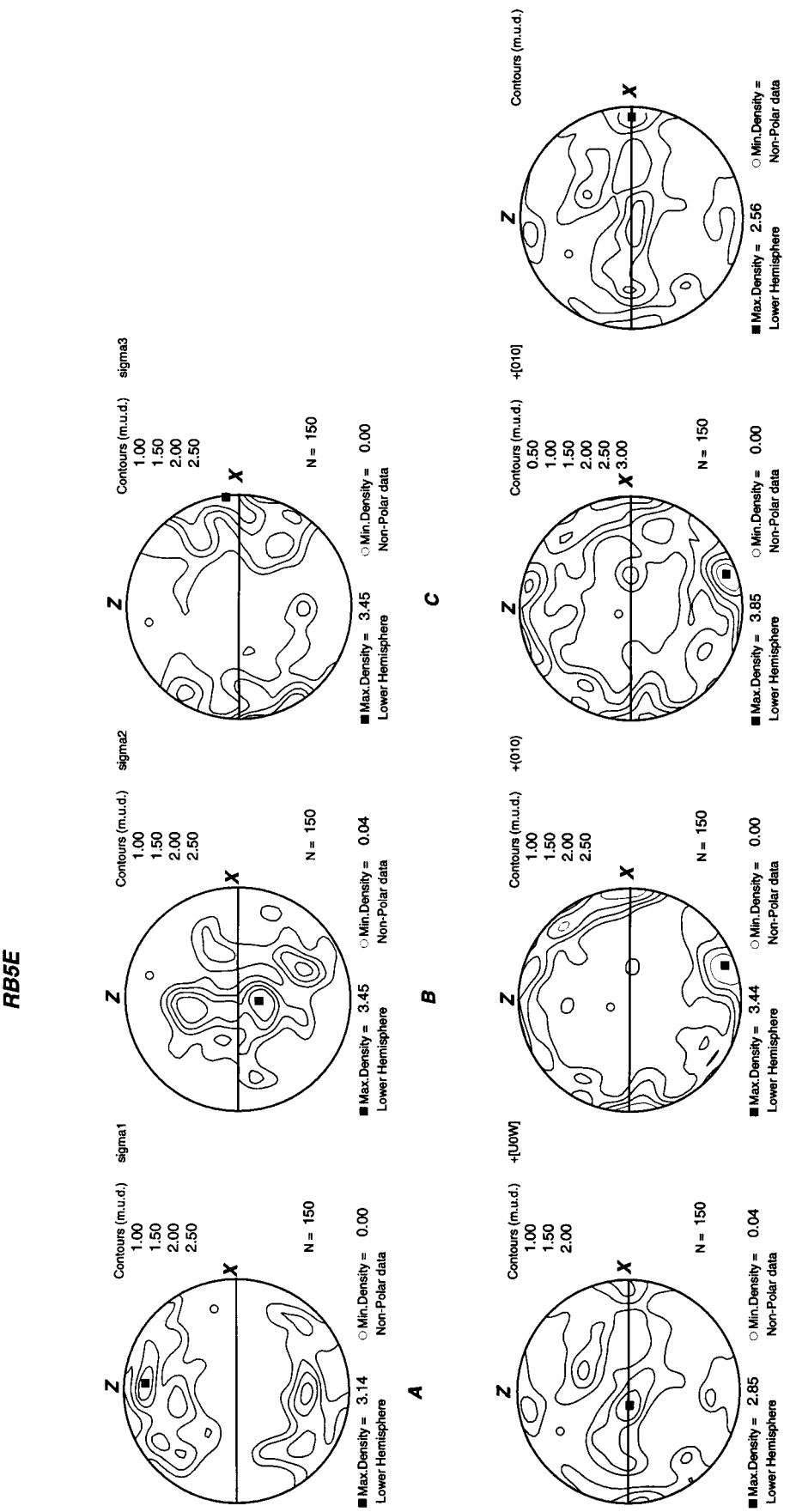


Fig. 17. Statistical distribution diagrams of the stress directions (A, B and C), albite and pericline directions (D and F), and albite and pericline planes (E and G) (sample RB5E).

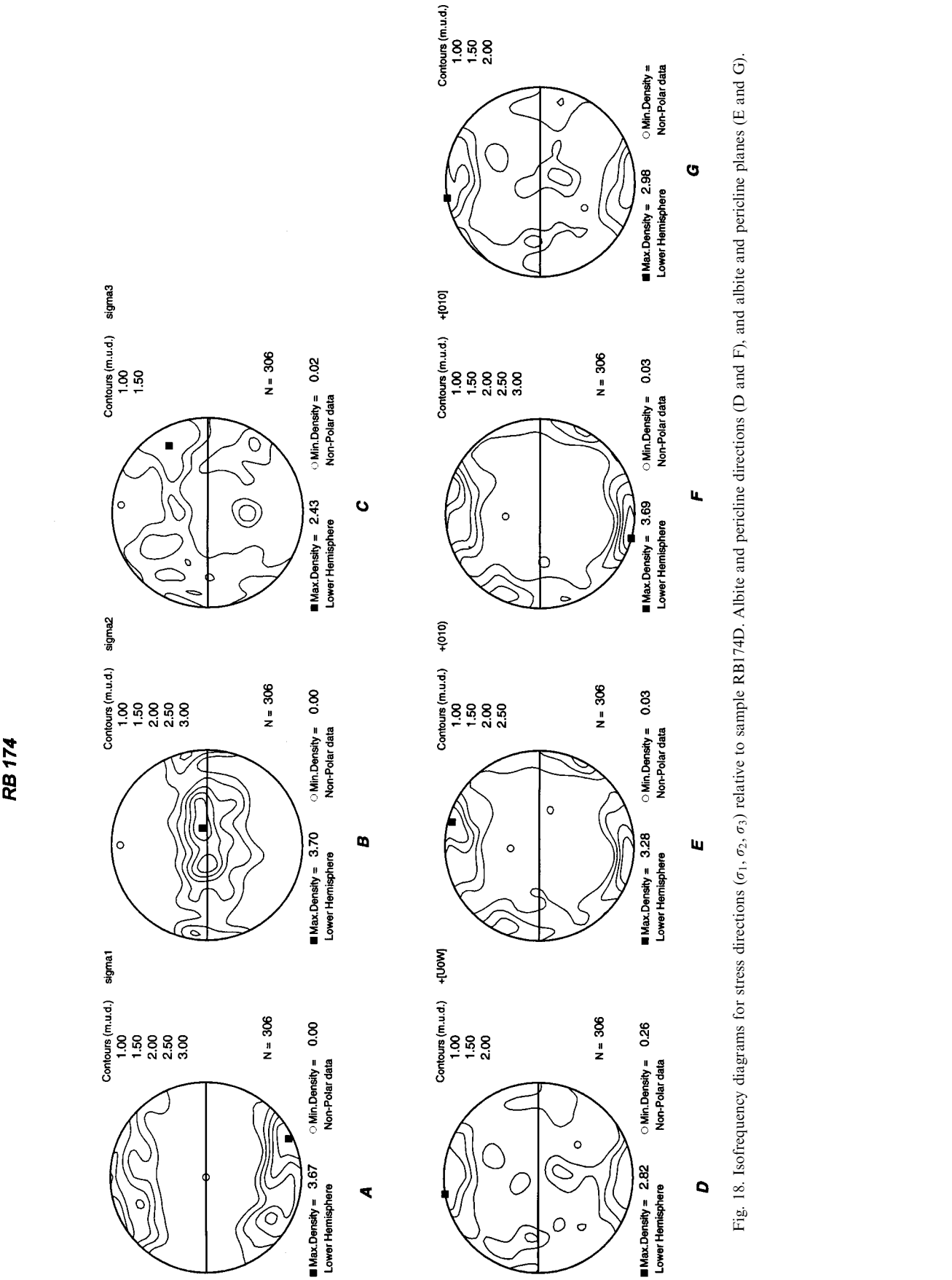


Fig. 18. Isofrequency diagrams for stress directions ($\sigma_1$, $\sigma_2$, $\sigma_3$) relative to sample RB174D. Albite and pericline directions (D and F), and albite and pericline planes (E and G).

2. (010) has a preferred orientation close to the pole of the foliation plane but there is a secondary maximum close to the X finite strain axes.
3. [001] directions do not have a regular pattern of distribution, they define girdles perpendicular or subparallel to the foliation plane with maxima near X or Z (Fig. 11C and F, respectively). The (001) poles from samples RB70 and 332 (Fig. 9C and F) show diffuse girdles which are subparallel to the YZ and XZ, planes and a strong concentration at 45° from X and Z and near X, respectively. These LPO patterns are similar to others previously reported in the literature (Olsen and Kohlstedt, 1985; Kruhl, 1987a, b; Ji and Mainprice, 1988, 1990; Ji et al., 1988).

Shelley (1979) has worked with volcanic metasedimentary rocks (hornblende–hornfels facies) and obtained LPO patterns with crystal *a* axes [100] lying on the bedding plane and with a maximum parallel to a lineation, which is the axis of greatest elongation or strain axis, and (010) parallel to the foliation. He suggested that this fabric was developed mimetically during the annealing of a previously igneous-type fabric. The distinctions from the LPO patterns we have obtained can be attributed to the differences in strain and metamorphic conditions in a high-temperature shear zone as well as a thermal (contact) metamorphism and consequently to the mechanisms that accounted for the development of a preferred crystallographic orientation.

The dynamic recrystallization process is an important mechanism for fabric development, in addition to lattice reorientation due to dislocation glide and/or twinning; however, little is known about the effect of dynamic recrystallization on fabric development (Urai et al., 1986).

As pointed out by Shelley (1986), several possible orientation mechanisms should be considered when attempting to explain the development of crystallographic-preferred orientation in plagioclases. However, under higher metamorphic conditions, i.e. high amphibolite and granulite facies, the ductility is greatly enhanced; consequently, intracrystalline slip is a potentially important mechanism (Olsen and Kohlstedt, 1984, 1986; Ji and Mainprice, 1988, 1990). The dislocations in intermediate plagioclase, which were deformed under granulite facies conditions, have been analysed by Olsen and Kohlstedt (1984) and this study has revealed extensive ductile deformation by intracrystalline slip and by twinning. The dominant slip system seems to be (010) [001].

We cannot ascribe only one orientation mechanism to LPO, but we believe that recrystallization-accommodated dislocation creep is the dominant mechanism of fabric development in our samples, i.e. intracrystalline slip and dynamic recrystallization. However, contribution from other mechanisms cannot be ruled out.

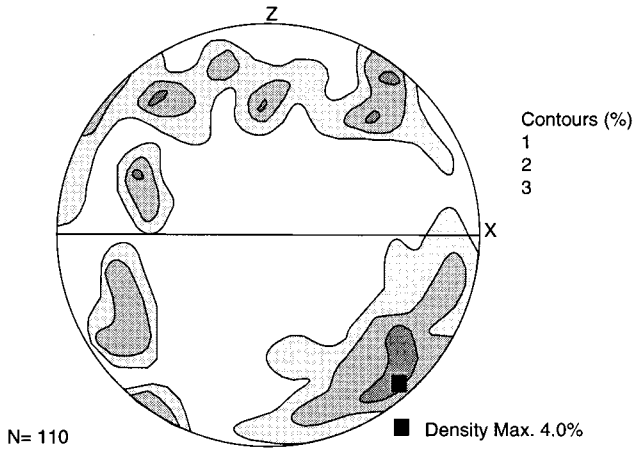


Fig. 19. Diagram of the stress directions from Lawrence's method (sample RB95).

### 8.2. Stress determination

A new method to determine stress directions has been applied to plagioclase mechanical twins, following the theoretical principles predicted and discussed by Borg and Heard (1970). The results are consistent for all studied samples, with the kinematics established from independent observations.

The stress directions determined are compatible with transcurrent movement in the southern portion of the area, where the intermediate compressive stress ($\sigma_2$) is vertical, and with inverse faults in the north.

Lawrence (1970) used the albite twinning of plagioclases to determine stress directions. We have also used this methodology to compare Lawrence's work with our results, and the sample RB95 has been chosen to test the Lawrence's method. Fig. 19 shows the maximum compressive stress ($\sigma_1$) orientation patterns obtained from the Lawrence's method, which is very similar to the one we have obtained using our method (Fig. 15). There are two advantages to this new technique. First, the determination of the orientation of the stress axes and of the albite and pericline planes is automatic. Second, our method can be used on plagioclases of any composition; Lawrence's method depends on correlating the crystallographic axes with the refractive index, which restricts the use of this method to plagioclases with An < 30.

We have distinguished two paleostress regimes: (a) the direction of maximum compressive stress oblique to regional foliation; and (b) the trends of the compressional directions normal to the foliation plane (Fig. 4). In the first case, the $\sigma_1$ direction is consistent with the fabric asymmetry and the dextral regional

shear movement, therefore, the fabric and the shear zone should be formed at the same time. However, in the second case of compression normal to foliation, we have two possibilities: it is a late compression at high temperature with plastic deformation and twinning of plagioclases; or a transpressional regime with a high normal stress but no movement.

From a geometrical and deformational point of view, field and fabric data are consistent with a transpressional regime, where pure shear is the most important tectonic regime, but locally the simple shear may take an important role. Our conclusion is supported by LPO orientations of plagioclase which have weak asymmetry mainly due to the maximum stress orientation (subparallel to Z) determined from mechanical twins.

## Acknowledgements

This research was supported by the Fundação de Amparo à Pesquisa do Estado de São Paulo (FAPESP, project. 95/0283-3) and USP/COFECUB (project 28/96). We thank Drs Alain Vauchez and João Hippertt for useful discussions and critical reading of an early version of this paper. Comments by Eric Tohver greatly improved the manuscript. We also thank Dr. Gianna M. Garda, for the English review, and Mauro Cesar Prado, undergraduate geology student and CNPq fellowship, for fabric measurements of some samples. We would like to thank the reviewers, Dr. D. Shelley and Dr. J.H. Kruhl.

## References

Benn, K., Mainprice, D., 1989. An interactive program for determination of plagioclase crystal axes orientations from U-stage measurements: an aid for petrofabric studies. Computers and Geosciences 15, 1127–1142.

Borg, I., Handin, J., 1966. Experimental deformation of crystalline rocks. Tectonophysics 3, 249–358.

Borg, I., Heard, H.C., 1970. Experimental and Natural Rock Deformation. Ed. P. Paulitsch. Springer-Verlag, Berlin pp. 375–403.

Buerger, M.J., 1945. Genesis of twin crystals. American Mineralogy 30, 469–482.

Burri, C., Parker, R.L., Wenk, E., 1967. Die optische Orientierung der Plagioklase. Birkhäuser, Basel.

Carter, N.L., Raleigh, C.B., 1969. Principal stress directions from plastic flow in crystals. Geological Society of America Bulletin 80, 1231–1264.

Davis, G.H., Reynolds, S.J., 1996. Structural Geology of Rocks and Regions, 2nd ed. John Wiley, New York.

Emmons, R.C., Gates, R.M., 1943. Plagioclase twinning. Geological Society of America Bulletin 54, 287–303.

Fernandes, L.A.D., Porcher, C., Egydio-Silva, M., Vauchez, A., 1996. Structural evolution and temperature conditions along a high-grade shear zone in SE Brazil. An International Conference on Structure and Properties of High Strain Zones in Rocks, Verbania, Italy (September 3–7). Abstract Volume Supplemento 107, p. 61.

Gay, P., Bown, M.G., 1956. The structures of the plagioclase feldspar—the heat treatment of intermediate plagioclase. Mineralogical Magazine 31, 306–313.

Ji, S., Mainprice, D., 1988. Natural deformation fabrics of plagioclase: implications for slip systems and seismic anisotropy. Tectonophysics 147, 145–163.

Ji, S., Mainprice, D., 1990. Recrystallization and fabric development in plagioclase. Journal of Geology 98, 65–79.

Ji, S., Mainprice, D., Boudier, F., 1988. Sense of shear in high temperature movement zones from the fabric asymmetry of plagioclase feldspar. Journal of Structural Geology 10, 73–81.

Ji, S., Zhao, X., Zhao, P., 1994. On the measurement of plagioclase lattice preferred orientations. Journal of Structural Geology 16, 1711–1718.

Kruhl, J.H., 1987a. Preferred lattice orientations of plagioclase from amphibolite and greenschist facies rocks near the Insubric Line (Western Alps). Tectonophysics 135, 233–242.

Kruhl, J.H., 1987b. Computer-assisted determination and presentation of crystallographic orientations of plagioclase, on basis of universal-stage measurements. Neues Jahrbuch für Mineralogie Abhandlung 157, 185–206.

Laurent, P., Tourneret, C., 1990. Determining deviatoric stress tensors from calcite twins: Applications to monophased synthetic and natural polycrystals. Tectonics 9, 379–389.

Lawrence, R.D., 1970. Stress analysis based on albite twinning of plagioclase feldspars. Geological Society of America Bulletin 81, 2507–2512.

Muir, I.D., 1955. Transitional optics of some andesines and labradorites. Mineralogical Magazine 30, 545–568.

Olsen, T.S., Kohlstedt, D.L., 1984. Analysis of dislocations in some naturally deformed plagioclase feldspars. Physics and Chemistry of Minerals 11, 153–160.

Olsen, T.S., Kohlstedt, D.L., 1985. Natural deformation and recrystallization of some intermediate plagioclase feldspars. Tectonophysics 11, 107–131.

Olsen, T.S., Kohlstedt, D.L., 1986. Natural deformation and recrystallization of some intermediate plagioclase feldspars—Reply. Tectonophysics 124, 363–364.

Pedrosa-Soares, A.C., Noce, C.M., Vidal, P., Monteiro, R.L.B.P., Leonardos, O.H., 1992. Toward a new tectonic model for the Late Proterozoic Araçuaí (SE Brazil)–West Congolian (SW Africa) Belt. Journal of South American Earth Sciences 6, 33–47.

Porcher, C.C., Fernandes, L.A.D., Egydio-Silva, M., Vauchez, A., 1995. Dados preliminares do metamorfismo M1 da Faixa Ribeira: Região de Três Rios e Santo Antônio de Pádua (RJ). V Simp. Estudos Tectônicos, Gramado (RS). Boletim de Resumos, 71–73.

Shelley, D., 1979. Plagioclase preferred orientation, Foreshore Group metasediments, Bluff, New Zealand. Tectonophysics 58, 279–290.

Shelley, D., 1986. Natural deformation and recrystallisation of some intermediate plagioclase feldspar—a discussion on preferred orientation development. Tectonophysics 124, 359–364.

Smith, J.V., Brown, W.L., 1988. Feldspar Minerals. Crystal Structures, Physical, Chemical, and Microtextural Properties. Springer-Verlag, Berlin.

Söllner, F., Lammerer, B., Weber-Diefenbach, K., 1991. Die krustenentwicklung in der küstenregion nördlich von Rio de Janeiro/Brasilien. Münchner Geologische Helfe 4, 1–101.

Tourneret, C., Laurent, P., 1990. Paleo-stress orientations from calcite twins in the North Pyrenean foreland, determined by the Etchecopar inverse method. Tectonophysics 180, 287–302.

Trompette, R., Uhlein, A., Egydio-Silva, M., 1992. The Brasiliano São Francisco cráton revisited (central Brazil). Journal of South American Earth Sciences 6, 49–57.

Trompette, R., 1994. Geology of Western Gondwana (2000–500 Ma). Pan-African–Brasiliano Aggregation of South America and Africa. Balkema, Rotterdam.

Turner, F.J., 1953. Nature and dynamic interpretation of deformation lamellae in calcite of three marbles. American Journal of Science 251, 276–298.

Urai, J.L., Means, W.D., Lister, G.S., 1986. Dynamic recrystallization of minerals. In: Hobbs, B.E., Heard, H.C. (Eds.), Mineral and Rock Deformation: Laboratory Studies: The Paterson Volume. Geophysical Monograph 36, pp. 161–199.

Vauchez, A., Tommasi, A., Egydio-Silva, M., 1994. Self-indentation of a heterogeneous continental lithosphere. Geology 22, 967–970.

Wenk, H.R., Bunge, H.J., Jansen, E., Pannetier, J., 1986. Preferred orientation of plagioclase-neutron diffraction and U-stage data. Tectonophysics 126, 271–284.